Manuscript prepared for Geosci. Model Dev. Discuss.
with version 2015/04/24 7.83 Copernicus papers of the LaTeX class copernicus.cls.
Date: 29 May 2015

^{14}C-age tracers in global ocean circulation models

W. Koeve, H. Wagner, P. Kähler, and A. Oschlies

GEOMAR Helmholtz-Zentrum für Ozeanforschung Kiel, Kiel, Germany

Correspondence to: W. Koeve (wkoeve@geomar.de)

Abstract

The natural abundance of ^{14}C in total CO_2 dissolved in seawater is a property applied to evaluate the water age structure and circulation in the ocean and in ocean models. In this study we use three different representations of the global ocean circulation augmented with a suite of idealised tracers to study the potential and limitations of using natural ^{14}C to determine water age, which is the time elapsed since a body of water was in contact with the atmosphere. We find that, globally, bulk ^{14}C-age is dominated by two equally important components, one associated with aging, i.e. the time component of circulation, and one associated with a "preformed ^{14}C-age". This latter quantity exists because of the slow and incomplete atmosphere/ocean equilibration of ^{14}C particularly in high latitudes where many water masses form. In the ocean interior preformed ^{14}C-age behaves like a passive tracer. The relative contribution of the preformed component to bulk ^{14}C-age varies regionally within a given model, but also between models. Regional variability in the Atlantic Ocean is associated with the mixing of waters with very different end members of preformed ^{14}C-age. Here, variations in the preformed component over space and time mask the circulation component to an extent that its patterns are not detectable from bulk ^{14}C-age. Between models, the variability of age can also be considerable (factor of 2), related to the combination of physical model parameters, which influence circulation dynamics or gas exchange. The preformed component was found to be very sensitive to gas exchange and moderately sensitive to ice cover. In our model evaluation, the choice of the gas exchange constant from within the currently accepted range of uncertainty had such a strong influence on preformed and bulk ^{14}C-age that if model evaluation would be based on bulk ^{14}C-age it could easily impair the evaluation and tuning of a model's circulation on global and regional scales. Based on the results of this study, we propose that considering preformed ^{14}C-age is critical for a correct assessment of circulation in ocean models.

1 Introduction

Coupled global ocean circulation models are often-used tools in studying the role of the oceans under a changing climate. They are, for example, used to predict future changes of ocean biogeochemistry. In this context, the time elapsed since the last contact of a water parcel with the atmosphere is of particular interest in order to understand the interaction of changes in climate, circulation and biogeochemical processes. A variety of tracers can be used to evaluate circulation and water age structure both in the real ocean and in biogeochemical ocean models (e.g. Lynch-Stieglitz, 2003). One tracer, ^{14}C-DIC, has become pivotal in such studies (Stuiver et al., 1983; Toggweiler et al., 1989; Jain et al., 1995; Caldeira et al., 2002; Matsumoto et al., 2004; Cao and Jain, 2005; Matsumoto, 2007). ^{14}C is naturally produced in the upper atmosphere and enters the ocean via gas exchange. In the ocean's interior, there is no ^{14}C production, and radioactive decay with a half-life of 5730 yr reduces its concentration over time. This leads to a decrease of the $^{14}C/C$ ratio of dissolved inorganic carbon, which allows the computation of ^{14}C-ages (yr) of the respective water. The natural distribution of ^{14}C in the ocean is often expressed in a delta notation relative to the $^{14}C/C$ ratio of the atmosphere ($\Delta^{14}C = (R_o / R_a - 1) \cdot 1000$; R_o, R_a are the $^{14}C/C$ ratios of ocean and atmosphere (1890 AD, Stuiver and Polach, 1977), respectively). Surface water in equilibrium with the preindustrial atmosphere (1890 AD), ignoring isotope fractionation, would have a $\Delta^{14}C = 0$ ‰ and a ^{14}C-age of 0 yr. ^{14}C-DIC is widely used in model evaluation (Matsumoto et al., 2004) for two reasons. First, it can be directly measured in the ocean. Secondly it can be implemented at relatively low computational cost both into biogeochemical and ocean-circulation models.

Several issues complicate the use of natural ^{14}C for data-based evaluation of ocean-model circulation. First, there is the assumption of constant atmospheric ^{14}C-boundary conditions often applied in ocean model ^{14}C-experiments. On multi-millenial time scales, the atmospheric ^{14}C-production and level is by no means constant (Bard, 1988; Adkins and Boyle, 1997; Franke et al., 2008a, b). Secondly, there are significant man-made changes to the $^{14}C/C$ distribution in the atmosphere and the ocean. The invasion of fossil fuel CO_2,

almost devoid of ^{14}C, into the ocean reduces the $^{14}C/C$ ratio (the Suess Effect; Suess, 1955). On the other hand, ^{14}C-CO_2 from atmospheric nuclear-bomb testing in the 1950s and 1960s has strongly increased it (Rafter and Fergusson, 1957). The combination of both effects masks the natural distribution of $^{14}C/C$ in the ocean considerably, in particular in the upper ocean (e.g. Stuiver, 1980 and Fig. 1a). Thirdly, it is usually assumed that the transport of $^{14}C/C$ from the surface to the deep sea via sinking organic particles can be neglected (Fiadeiro, 1982; Jahn et al., 2014).

Finally, the time to reach ^{14}C-CO_2 equilibration between atmosphere and surface ocean is in the order of a decade (Broecker and Peng, 1974), which is longer than water residence time at the surface. In particular, the entrainment of old, ^{14}C-depleted water does not allow surface $^{14}C/C$ ratios to reach equilibrium with the atmosphere. Thus ^{14}C-ages in the surface ocean after correction for bomb-^{14}C are on the order of hundreds of years (Fig. 1b). Elevated surface ages have been confirmed by radiocarbon measurements in warm-water corals from periods before bomb testing or before the industrial era (e.g. Druffel, 1981) which shows that they are not an artefact of the corrections for bomb-^{14}C or the Suess effect. Surface water sinking into the interior of the ocean in high latitudes, however, is known to have an initial ^{14}C-age up to 900 yr older than tropical and subtropical surface waters (Bard, 1988). Hence ^{14}C-ages in the interior ocean are not real circulation ages. They are not solely reflecting the passage time in the interior of the ocean, but are apparent ages only (e.g. Broecker, 1979).

In the context of ocean biogeochemistry the time elapsed since the last contact of a water parcel with the atmosphere, i.e. when it is assigned zero age, is of particular interest. For example, the estimation of rates of ocean respiration or $CaCO_3$-dissolution from cumulative tracer changes (Sarmiento et al., 1990; Broecker et al., 1991; Feely et al., 2002) requires reliable age determinations. ^{14}C-ages of several hundred years for waters actually in contact with the atmosphere can thus pose a severe problem. Inferring true ages from ^{14}C-ages in the interior of the ocean obviously requires a correction for the "initial-age" effect before they can be used to derive the time component of circulation (Broecker, 1979; Bard, 1988; Campin et al., 1999). The term "bulk ^{14}C-age" (^{14}C-age^{bulk}) is used here to denote ages

computed from the distribution of natural ^{14}C-DIC not corrected for the initial, preformed ^{14}C-DIC. We use the terms "preformed" ^{14}C-DIC and "preformed" ^{14}C-age (Emerson and Hedges, 2008) in analogy to preformed components of other ocean tracers such as nutrients, oxygen or alkalinity (Redfield et al., 1963, Najjar et al., 2007, Koeve et al., 2014). The common feature of bulk tracers is that their distribution within the ocean's interior is a combination of a preformed component entering the ocean interior via physical transport processes (subduction, downwelling), a component related to processes (sources or sinks) within the ocean (respiration, remineralisation, mineral dissolution, radioactive decay), and the mixing of both components as water masses mix (Duteil et al., 2012, 2013; Koeve et al., 2014). Note that the term "reservoir age" is used in the radiocarbon and paleo-climatological literature in a similar way in which "preformed age" is used in this paper.

It is standard procedure to use Δ^{14}C or bulk ^{14}C-ages uncorrected for preformed ^{14}C from models and observations to evaluate model circulation (e.g. Matsumoto et al., 2004). In this study we present model experiments using ^{14}C-based tracers and a tracer of ideal age from three different ocean biogeochemical models. Our major objective is to gain insight into the magnitude and distribution of preformed ^{14}C-age both in models and in the real ocean. Further we will discuss how neglecting preformed ^{14}C-age and the use of bulk ^{14}C-ages may bias the assessment of ocean models and lead to a faulty tuning of the circulation in ocean models. A realistic model circulation, however, is not only prerequisite to a reliable climate prediction, it is also a critical aspect in biogeochemical or carbon cycle model studies. Unrecognized issues in the model physics may give rise to a faulty tuning of biogeochemical processes, for example when bulk nutrient concentrations are used to evaluate a model's biogeochemistry (Duteil et al., 2012).

2 Methods and models

2.1 Models and modelling approach

We employ three different models, two of which use an offline approach and one is an online fully-coupled earth-system model. For the offline models we use the transport matrix method (TMM) described in detail by Khatiwala et al. (2005) and Khatiwala (2007). In this approach ocean-tracer transport is represented by a matrix operation involving the tracer field and a transport matrix extracted from a global circulation online model (Khatiwala, 2007). In particular, we use two matrices extracted from two versions of the MIT general circulation model, a state-of-the-art primitive-equation model (Marshall et al., 1997). The coarse-resolution matrix (hereafter MIT2.8) was derived from a $2.8^\circ \times 2.8^\circ$ global configuration of this model with 15 vertical layers, forced with monthly mean climatological fluxes of momentum, heat, and freshwater, and subject to a weak restoring of surface temperature and salinity to observations. The higher resolution matrix (hereafter ECCO) is based on the data-assimilation model of the ECCO-consortium (Estimating the Circulation and Climate of the Ocean; Stammer et al., 2004) and has a horizontal resolution of $1^\circ \times 1^\circ$ and 23 vertical layers. For details see Khatiwala (2007) and Kriest et al. (2010, 2012). Wind-speed dependence of gas exchange applies winds from Trenberth et al. (1989) with a monthly resolution regridded to the respective model grid. Sea-ice fields applied are the OCMIP-2 ice mask (Orr et al., 1999) for MIT2.8 and NASA ISLSCP climatology (http://iridl.ldeo.columbia.edu/SOURCES/.NASA/.ISLSCP/.GDSLAM/.Snow-Ice-Oceans/.sea/.sea_ice/) for ECCO (S. Dutkiewics, MIT, personal communication, 2011). OCMIP is the Ocean Carbon cycle Model Intercomparison Project (http://ocmip5.ipsl.jussieu.fr/OCMIP/).

The third model used is the University of Victoria Earth System Climate Model (UVIC; Weaver et al., 2001), version 2.8 in the configuration used at GEOMAR (Oschlies et al., 2008). The ocean component of this model is a coarse-resolution ($1.8^\circ \times 3.6^\circ$, 19 vertical layers) 3-D-ocean general-circulation model (MOM2). Wind velocities are prescribed from the NCAR/NCEP monthly climatology. Sea-ice coverage is computed from a dy-

namic/thermodynamic sea-ice model (Bitz et al., 2001). The biogeochemical ocean model of the UVIC is described in detail by Schmittner et al. (2008).

For the ^{14}C-simulations with the TMM models we largely follow the OCMIP-2 protocol (Orr et al., 1999; Jahn et al., 2014) and study the natural ^{14}C-distribution in an abiotic setting and against an atmosphere of $\Delta^{14}C = 0$ and a constant $p\mathrm{CO}_2^{\mathrm{atm}} = 280\,\mu\mathrm{atm}$. DIC and ^{14}C-DIC are prognostic model tracers of total dissolved inorganic carbon and its ^{14}C-isotope, respectively. Alkalinity is prescribed from the model's salinity field assuming a fixed alkalinity / salinity ratio. OCMIP-2 ^{14}C-simulations are abiotic model runs, biotic fluxes of ^{14}C (as well as of DIC and alkalinity) are ignored following Fiadeiro (1982). Also the effect of isotope fractionation is not considered. Our notation of Δ^{14}C follows the OCMIP2 protocol (Orr et al., 1999).

All model runs were integrated for several thousand years (for details see Section 3) and can be considered equilibrium runs. For UVIC the ^{14}C-simulations can be made alongside a biotic model run (Schmittner et al., 2008).

Air–sea exchange of CO_2 and $^{14}CO_2$ in all three models is treated according to Eqs. (1) and (2).

$$\mathrm{CO_2\,(ex)} = (1 - \mathrm{ice}) \cdot k_{\mathrm{w}} \cdot (\mathrm{CO^*_{2(water)}} - \mathrm{CO^*_{2(air)}}) \tag{1a}$$

$$^{14}\mathrm{CO_2\,(ex)} = (1 - \mathrm{ice}) \cdot k_{\mathrm{w}} \cdot (\mathrm{CO^*_{2(water)}} \cdot R_{\mathrm{(water)}} - \mathrm{CO^*_{2(air)}} \cdot R_{\mathrm{(atm)}}) \tag{1b}$$

$$k_{\mathrm{w}} = a \cdot U^{\mathrm{n}} \cdot (Sc/660)^{-\eta} \tag{2}$$

with $\mathrm{CO^*_{2(air)}} = \mathrm{CO_{2\,(sol)}} \cdot p\mathrm{CO_{2\,(atm)}} \cdot P_{\mathrm{(atm)}}$.

k_{w} is the gas transfer velocity, U is wind speed, $n = 2$, *Sc* is the Schmidt number, and $\eta = 0.5$. $\mathrm{CO^*_{2(water)}}$ is the sum of CO_2 dissolved in seawater and H_2CO_3 in surface water computed from the DIC concentration and an estimate of pH (e.g. Follows et al., 2006). $\mathrm{CO^*_{2(air)}}$ is the equilibrium CO_2 concentration given atmospheric $p\mathrm{CO_2}$, CO_2 solubility, and the local atmospheric pressure; $\mathrm{CO_{2\,(sol)}}$ is the solubility of CO_2, $p\mathrm{CO_{2\,(atm)}}$ is CO_2 partial pressure in the atmosphere, $P_{\mathrm{(atm)}}$ is the local atmospheric pressure, $R_{\mathrm{(atm)}}$ is the $^{14}\mathrm{C}\,/\,\mathrm{C}$ ratio of the atmosphere and $R_{\mathrm{(water)}}$ is the $^{14}\mathrm{C}\,/\,\mathrm{C}$ ratio of the surface water. In the standard

configuration the gas transfer velocity k_w is computed using a value of $a = 0.337$, following the OCMIP-2 protocol. The term "ice" represents the fraction of water area covered by sea ice.

In the ocean, bulk ^{14}C-age (in units of years) can be computed (Stuiver and Polach, 1977) according to Eq. (3):

$$^{14}\text{C-age} = -8267 \log_e(\Delta^{14}\text{C}/1000 + 1) \quad (3)$$

2.2 Model tracers

In order to study the distribution of preformed ^{14}C in the interior of the ocean, we design a suite of additional model tracers.

1. ^{14}C-DIC$^{\text{bulk}}$: this is the tracer of natural ^{14}C-DIC implemented following the OCMIP2 protocol. The age computed from this tracer via Eq. (3) has also been called "conventional ^{14}C-age" (Khatiwala et al., 2012) but is usually referred to as "^{14}C-age" or "radiocarbon age". We will use the term ^{14}C-age$^{\text{bulk}}$ in order to highlight the fact that it consists of several components (see below).

2. age$^{\text{ideal}}$: a tracer of the time elapsed since the last contact with atmosphere. The "ideal age" model tracer (Thiele and Sarmiento, 1990; England, 1995; England and Maier-Reimer, 2001) works like a clock counting time after being restored to zero, which happens every time the water resides at the surface. Everywhere else it ages with a rate of 1 day day^{-1} and is subject to mixing and advection in the interior of the ocean. Synonyms of the age measured by this tracer used in the scientific literature include: "circulation age" (Matsumoto, 2007; Khatiwala et al., 2012), "ventilation age" (Adkins and Boyle, 1997; Campin et al., 1999), and "ideal age" (Thiele and Sarmiento, 1990).

3. ^{14}C-DIC$^{\text{pre}}$: a preformed ^{14}C-DIC tracer is restored to the model's actual ^{14}C-DIC at the surface while in the interior of the ocean it is only mixed and advected but is not

subject to radioactive decay. The respective preformed ^{14}C age (yr) is computed from $^{14}\text{C-age}^{\text{pre}} = -8267 \cdot \log_e(^{14}\text{C-DIC}^{\text{pre}} / \text{DIC}^{\text{pre}})$, where DIC^{pre} is preformed total CO_2. Note that in an abiotic run DIC^{pre} is always equal to DIC. The term "reservoir age" has been used synonymously (Khatiwala et al., 2012 and references therein).

4. $^{14}\text{C-DIC}^{\text{decay}}$: a ^{14}C-DIC-decay tracer is set to zero in surface waters and numerically integrates ^{14}C-decay of the ^{14}C-DIC tracer in the interior of the ocean. It is also advected and mixed in the interior of the ocean. The ^{14}C-decay age (yr) is computed from $^{14}\text{C-age}^{\text{decay}} = -8267 \cdot \log_e[(\text{DIC} + {}^{14}\text{C-DIC}^{\text{decay}}) / \text{DIC}]$.

5. age^{pre}: in order to simplify the comparison between the ideal-age tracer and the age computed from the ^{14}C-DIC tracer, we design another tracer of preformed ^{14}C-age. This tracer (age^{pre}) has units of time. At the surface it is assigned the bulk ^{14}C-age, which is computed at any time step during model runtime from $^{14}C / C$ ratios. In the interior of the ocean this tracer is advected and mixed like all other tracers, but it does not age. While tracer $^{14}\text{C-DIC}^{\text{pre}}$ (3) is one of concentration, age^{pre} is one of time.

6. age^{bulk}: finally, we design an explicit tracer which combines the behaviour of the age^{pre} tracer at the surface and the ideal age tracer ($\text{age}^{\text{ideal}}$) in the interior of the ocean. At the surface age^{bulk} is assigned the bulk ^{14}C-age, which is computed at any time step during model runtime from $^{14}C / C$ ratios. In the ocean interior it ages with a rate of $1\,\text{day}\,\text{day}^{-1}$ and is subject to mixing and advection.

This provides us with a duplicate set of tracers (Table 1) describing the preformed component, the circulation component, and bulk. One set of the tracers is based on ^{14}C, the other on age. The complete set of tracers is presented and discussed for ECCO-model simulations. The tracers $^{14}\text{C-DIC}^{\text{bulk}}$ and $\text{age}^{\text{ideal}}$ are implemented in all three models. The detailed experimental setups are presented together with the results in Section 3.

3 Principal components of bulk ^{14}C age

3.1 Ideal age and bulk ^{14}C-age distribution in three ocean models and the concept of preformed ^{14}C-age

Reference model runs (10000 yrs) are carried out with all three models. We apply a gas transfer constant of $a = 0.337$, wind fields and ice cover as given in Section 2.1 for these runs. Implemented tracers are DIC, ^{14}C-DIC^{bulk} and age^{ideal}. We use these tracers to approximate the preformed component of ^{14}C-age^{bulk} in the different models by diagnosing it during post processing from the difference of ^{14}C-age^{bulk} and age^{ideal}. Reference runs also serve as spin-up runs from which other model experiments are initialised.

To start with, we compare global mean profiles of ^{14}C-age^{bulk} and age^{ideal} (Fig. 2a). A number of features is evident. First, ^{14}C-age^{bulk} is much larger than age^{ideal} in any model. The global mean offset between the two age measures varies by up to a factor of two between models (Fig. 2b). In the deep ocean the offset is about 400 yr in MIT2.8 and 680 yr (800 yr) in ECCO (UVIC), respectively. The age offset may be either rather homogeneous vertically (MIT2.8) or have a marked vertical gradient of up to 400 yr difference between surface and deep water (ECCO and UVIC). Secondly, global mean surface ^{14}C-age^{bulk} is smaller than the data-based estimate from GLODAP in all three models (Fig. 2a). Thirdly, a judgement based just on global mean profiles of ^{14}C-age^{bulk} would indicate that over most of the ocean the UVIC model is the one in best agreement with observations. Furthermore, one might conclude that the MIT2.8 model appears to have too young waters and presumably too vigorous a circulation almost everywhere.

Interestingly, the age^{ideal} tracer indicates just the opposite. Deep-ocean MIT2.8 waters have highest ages pointing to a more sluggish circulation while in UVIC (and ECCO) deep-ocean waters are in fact younger, indicating a more vigorous circulation compared to the MIT2.8 model. Finally, in the upper 2000 m, the global mean profiles of the ideal age tracer suggest the circulations to be similar in all three models, at least much more similar than indicated by ^{14}C-age^{bulk}.

In conjunction with the observations that ocean/atmosphere ^{14}C-equilibration is slow (Broecker and Peng, 1974) and surface-ocean ^{14}C-age^{bulk} is well above zero (see Fig. 1b), we suspect that (most of) the difference between ^{14}C-age^{bulk} and age^{ideal} in the interior of the ocean is due to the ^{14}C-age^{bulk} which a water mass had at the time when entering the ocean's interior, i.e. its preformed ^{14}C-age.

In Fig. 3, we present the large-scale distribution of ^{14}C-age^{bulk} and age^{ideal} from the ECCO model run along sections through the Atlantic Ocean (20° W) and the Pacific Ocean (140° W). Surface ^{14}C-age^{bulk} is around 200 yr in the subtropical ocean basins, around 300 yr in the North Atlantic and around 1000 yr in the Southern Ocean. In the interior of the ocean, ^{14}C-age^{bulk} increases from about 300 yr in the northern North Atlantic Ocean almost continuously along the path of circulation originally proposed for the global conveyor-belt by Broecker and Peng (1982) towards the deep northern North Pacific where ^{14}C-age^{bulk} is about 2000 yr (Fig. 3a). In contrast, age^{ideal} (Fig. 3b) is zero all over the surface ocean, and close to zero in the deep waters of the two major ocean ventilation regions, i.e. the northern North Atlantic and the Southern Ocean (Marshall and Speer, 2012). Elevated age^{ideal} is found in the deepest waters of the Atlantic Ocean (700 yr) and in particular towards the northern North Pacific where maximum ages are around 1400 yr along the transect chosen. Basin-scale patterns of age^{ideal} and ^{14}C-age^{bulk} are similar in the Pacific mainly due to a very homogeneous N–S distribution of preformed age (Fig. 3c). In the Atlantic Ocean, however, the strong N–S gradient in preformed age masks important aspects of circulation in the ^{14}C-age^{bulk} distribution. For example, the continuous north-to-south increase in the ^{14}C-age^{bulk} is not consistent with the strong ventilation in the Southern Ocean, but is mainly governed by waters of large preformed ^{14}C-age subducting in the Atlantic Sector of the Southern Ocean.

The preformed age shown in Fig. 3c is taken from the age^{pre} tracer (Table 1). The sum of age^{ideal} and this preformed age tracer agrees with the ^{14}C-age^{bulk} within a few percent (see Fig. 3d for the residual). As we will explain and quantify in the following section, the

residual derives from a non-linear effect of ^{14}C-DIC and DIC tracer mixing on computed age. To reflect this we write Eq. (4):

$$^{14}\text{C-age}^{\text{bulk}} = \text{age}^{\text{ideal}} + {}^{14}\text{C-age}^{\text{pre}} + \text{“mixing residual”} \quad (4)$$

3.2 Effects of tracer mixing on age estimates

In the following we will use dedicated model experiments carried out with the ECCO model, in order to quantify the relative importance of the three terms on the right-hand side of Eq. (4). We implement DIC and all six tracers described in Section 2.2. We will use this combination of tracers to quantify the non-linearity arising from mixing of the ^{14}C-DIC and DIC tracers on computed ^{14}C-age components. To explore the effect of tracer mixing on ^{14}C-ages in more detail, we first apply the additional tracers ^{14}C-DIC$^{\text{pre}}$ and ^{14}C-DIC$^{\text{decay}}$ (Table 1). We initialize these tracers from model output of the spin-up run (after 4000 yrs) with the DIC, ^{14}C-DIC and age$^{\text{ideal}}$ tracers assuming the “mixing residual” term of Eq. (4) to be zero everywhere. Running the model for another 6000 yr, we find the sum of the preformed and the decay tracers to match the ^{14}C-DIC tracer perfectly (Fig. 4a). The sum of ages (^{14}C-age$^{\text{pre}} + {}^{14}$C-age$^{\text{decay}}$), however, is smaller by 6 % on average than the age computed from the ^{14}C-DIC$^{\text{bulk}}$ tracer (Fig. 4b).

The difference between Fig. 4a and b, i.e. the low bias in ages computed from ^{14}C-tracers relative to the tracer itself, is explained by the combination of the logarithmic transformation in the age computation (Eq. 3) and the effect of mixing of waters with different $^{14}\text{C}/\text{C}$ tracer ratios (Jenkins, 1987; Delhez et al., 2003; Khatiwala et al., 2001, 2012).

To make this effect visible and quantifiable in our model, we compare age estimates from two sets of tracers (Table 1) tracking (a) the circulation component of age, (b) preformed age, and (c) bulk age. One set of these tracers behaves ideally in the interior of the ocean, in the sense that where they are affected by mixing, the mixing products can be described by mixing along a linear mixing line. These tracers are the age$^{\text{ideal}}$, age$^{\text{pre}}$, and age$^{\text{bulk}}$ tracers (Table 1). The latter two tracers inherit the age of ^{14}C-age$^{\text{bulk}}$ at the surface, while in the

interior of the ocean they behave like ideal tracers, being either only transported (age^{pre} tracer) or being both transported and aging with a rate of 1 day day^{-1} (age^{bulk} tracer). We compare ages derived from these ideally-behaving tracers and the respective ages from the ^{14}C-based tracers, ^{14}C-age^{decay}, ^{14}C-age^{pre}, and ^{14}C-age^{bulk}. In all three cases (circulation component of age, preformed component of age and bulk age) we see that ^{14}C-based ages underestimate their ideally-behaving counterparts. We present the results as anomalies (ideally behaving – ^{14}C-based) of ages along the combined section through the Atlantic (30° W), Southern (60° S) and Pacific (140° W) Oceans (Fig. 5). The age anomaly $age^{bulk} - {}^{14}$C-age^{bulk} (Fig. 5a) is close to zero in the surface ocean, in the northern North Atlantic, and in the Atlantic sector of the Southern Ocean. Away from these outcrop regions and largely following increasing ideal age (age^{ideal}) the anomaly increases to maximum values of about 50 yr in the (South) Atlantic Ocean and about 80 yr in the (North) Pacific Ocean. This difference is moderate and equivalent to a few percent of ^{14}C-age^{bulk}. Preformed ages (Fig. 5b) show very small anomalies ($age^{pre} - {}^{14}$C-age^{pre}) of only a few years (and usually less than 1 % of age^{pre}), again with maxima in the South Atlantic Ocean and the North Pacific Ocean. The largest difference is found between age^{ideal} and ^{14}C-age^{decay}. In the deep northern North Pacific this difference is almost 200 yr (Fig. 5c). Over much of the Pacific Ocean it is equivalent to about 15 % of ideal age.

The effect of non-linear mixing on ^{14}C-ages has been studied previously (Deleersnijder et al. 2001; Holzer et al., 2010; Khatiwala et al., 2012). Applying a boundary propagator approach (Holzer et al., 2010) Khatiwala et al. 2012 found a difference between their mean age (Γ) and their radiocarbon age (Γ_C) of usually less than 50 yrs, which is comparable to the overall effect of non-linear mixing (age^{bulk} - ^{14}C-age^{bulk}) (Fig. 6a) observed in our model, while the difference (age^{ideal} - ^{14}C-age^{decay}) from our model (Fig. 6c) is considerably larger. This may be explained by methodological differences. While our ^{14}C-age^{decay} is based on the numerical integration of ^{14}C-decay, the definition of the radiocarbon age, $^{14}C(x) = {}^{14}C_0(x)e^{\lambda\Gamma_C(x)}$, of Khatiwala et al. 2012 uses $^{14}C_0$ as the weighted average of the ^{14}C surface concentration.

The small difference age^{bulk} − ^{14}C-age^{bulk} (Fig. 5a) in combination with an almost perfect behaviour of the preformed-age tracers (Fig. 5b) suggests that our initial assumption (Section 3.1, Fig. 2) that the preformed age can be well approximated by (Eq. 5), i.e. the difference between the ^{14}C-age^{bulk} and age^{ideal} of a model, is justified.

$$^{14}\text{C-age}^{pre} \approx {}^{14}\text{C-age}^{bulk} - \text{age}^{ideal} \quad (5)$$

In any case, preformed ^{14}C-ages estimated from this difference provide a conservative, lower-limit estimate of preformed age. In the ECCO model, this underestimate may be as large as 20 % in individual grid boxes (Fig. 4c). On average, however, it is about 7 % with higher values observed towards the North Pacific Ocean. This uncertainty is small given the order of 50 % contribution of the preformed age to bulk ^{14}C-ages presented in Section 3.1. For the sake of saving computational time by having a reduced number of tracers, we hence ignore the mixing effect in the following section where we discuss a series of sensitivity runs.

3.3 Mechanisms controlling preformed ^{14}C-age

In this section we treat the major processes, which determine the magnitude of preformed ^{14}C-age, and how they influence model assessment if based on ^{14}C-age^{bulk}. We perform several sensitivity experiments to study the sensitivity of preformed ^{14}C-age distribution to relevant model parameters. All sensitivity experiments are carried out with the reduced set of model tracers (i.e. ^{14}C-DIC^{bulk} and ideal age tracer, Table 1) and we diagnose the preformed ^{14}C-age offline during post-processing of model output using Eq. (5). This procedure is justified by the results presented in Sect. 3.2.

^{14}C-age^{bulk} of several hundred years in the surface ocean (Fig. 1b) have been attributed to the long equilibration times of carbon isotopes (Broecker and Peng, 1974). While for CO_2 the equilibration time is governed by the product of the time scale of gas exchange (order of one month) and the ratio CO_3^{2-} / CO_2^{aq} (10–15 in the surface ocean), the equilibration time of carbon isotopes scales with the ratio TCO_2 / CO_2^{aq}. Since there is about ten times more total CO_2 than there are carbonate ions in seawater, the equilibration time of carbon isotopes is larger by about a factor of ten, i.e. on the order of a decade (Broecker and Peng,

1974). Elevated and variable ^{14}C-DIC^{bulk} in the surface ocean suggests that the residence time of waters at the ocean surface is usually much shorter than this equilibration time and equilibrium with atmospheric ^{14}C is therefore not attained. The actual residence time (Bolin and Rohde, 1973; Takeoka, 1984) of waters in the surface ocean is not well known though. Diagnosing the residence time of surface waters, and particularly its regional variations with respect to the observed distribution of ^{14}C-DIC^{bulk} at the surface, is not straightforward in our model. Instead, we take a first step into this direction and model the “reverse age" of the surface water, i.e. the time passed since its last stay below the surface layer. For this purpose we modify the definition of our ideal age tracer such that it is set to zero everywhere below a model specific reference depth and allowed to age in layers higher up. The reference depths are 135 m in ECCO and 120 m in MIT2.8. The idea here is to have a reference depth larger than 100 m, a depth often used pragmatically to define the productive surface layer. Differences between the reference depths are simply due to the different vertical resolutions in the models. The time passed since the last residence below the surface is henceforth referred to as the “surface water age" . In our MIT2.8 model, for example, surface water ages range up to two years in subpolar and most northern-hemisphere polar waters, up to five years in Southern Ocean polar waters and equatorial upwelling regions, and up to 7 years in the subtropical gyres (Fig. 6). In the ECCO model the surface water ages in the Southern Ocean are lower. In general, in areas of deep convection or upwelling surface water age is low while in areas characterized by horizontal advection and downwelling it is larger. Deep convection and upwelling are thus a continuous source of old waters low in ^{14}C to the surface ocean. Our estimates of the surface water age (Fig. 6) are qualitatively consistent with the observed distribution of ^{14}C-age^{bulk} at the surface (Fig. 1b). Regions with low surface water ages show high ^{14}C-age^{bulk}, and vice versa. Still, our surface water ages may be considered lower estimates of true residence or exposure time (Delhez et al., 2004) since the respective age tracer will be reset to zero each time a water parcel is below the reference depth, even if for a brief period only.

Most of the deep-ocean volume is ventilated from relatively small regions in the high latitudes. It is conditions in these regions, which control the preformed ^{14}C-age distribution in

the ocean's interior. One such region is the northern North Atlantic. Surface waters there origining mainly from the low-latitude Atlantic Ocean are to be converted into North Atlantic Deep Water (NADW). Source waters have been at or near the surface for several years allowing ^{14}C-DIC to approach equilibrium with the atmosphere. Furthermore, deep convection in the northern North Atlantic entrains relatively young waters into the surface each winter. Combined, both effects give rise to moderately negative surface $\Delta^{14}C$ and moderate ^{14}C-ages in the surface (Fig. 1b).

In the Southern Ocean the situation is different. Upwelling south of the Antarctic Polar Front brings very old waters to the surface. In fact, some of this water stems from the return flow of the global conveyor belt. Having left the ocean's surface in the northern North Atlantic it has travelled through the deep Atlantic Ocean, the Circumpolar Current system, further up to the North Pacific and back to the Southern Ocean isolated from the atmosphere all the time, which has been estimated to be in the order of 2700 yr (DeVries and Primeau, 2011). Other components of the water upwelling in the Southern Ocean have been ventilated relatively recently in the North Atlantic or have returned after a passage of about 2000 yr from the tropical Indian Ocean. Hence, waters upwelling in the Southern Ocean are in bulk much older and more depleted in ^{14}C-DIC, compared to those entering the deep-water formation regions at the surface of the North Atlantic. Combined with short surface residence times, this gives rise to much larger preformed ^{14}C-ages in the Southern Ocean deep-water formation regions, about 1000 yr in the real ocean (Bard, 1988; Fig. 1b).

Several factors could potentially influence the overall magnitude and distribution of preformed ^{14}C-age in models and the real ocean. These are (a) the intensity of upwelling in the Southern Ocean, (b) the rate of gas exchange, (c) ice coverage, (d) water residence time in the surface of the region of water mass formation, and (e) the relative contribution of different source water regions (e.g. NADW and AABW) to the total deep-water formation rate.

The gas-exchange formulation (Eqs. 1–3) is essentially identical in all three tested models. In particular the standard configurations of all models apply wind speed squared and the OCMIP2 gas-transfer constant of 0.337. This value is based on tuning one model of the

OCMIP2 family together with its given wind and sea ice fields against the bomb ^{14}C ocean inventory estimated from observations (Broecker et al., 1985) and considered correct at the time of the OCMIP2 experiment. Evidence has since accumulated suggesting the bomb ^{14}C ocean inventory to be in fact smaller by up to 25 % (Sweeney et al., 2007). As a consequence, the gas transfer constant may need a corresponding reduction. Such a change in the gas-transfer constant has little effect on net oxygen or total-CO_2 fluxes between ocean and atmosphere. It has, however, a considerable effect on $^{14}C\text{-age}^{pre}$ and hence also the $^{14}C\text{-age}^{bulk}$ distribution in the ocean. Using all models, we repeat the standard experiment with a reduced gas exchange rate. For this purpose we reduce the standard value of the gas transfer constant from $a = 0.337$ to a value of $a = 0.24$ (see Eq. 2). This change causes the global mean profiles of preformed ^{14}C-ages (Fig. 7a) to increase by about 150 (ECCO, UVIC) to 200 (MIT2.8) yr. In the global mean profile this shift is almost uniform with depth. Concerning the global mean profiles of $^{14}C\text{-age}^{bulk}$, two features are evident (Fig. 7b). First, model surface values are now ($a = 0.24$) much closer to bulk ages derived from the "observed" natural ^{14}C as compared to our reference runs ($a = 0.337$; Fig. 2a). Reducing the gas transfer constant hence solves one of the model-data comparison issues discussed in Sect. 3.1 (Fig. 2a). At depth (ignoring the deepest layers below 4000 m) this increase shifts the global mean profile of the MIT2.8 much closer to observations. With the reduced gas exchange constant $^{14}C\text{-age}^{bulk}$ of the UVIC model appear to be too large compared to observations and the ECCO model appears to be the best-performing model in our model intercomparison, except at the surface. ^{14}C-based judgement of model circulation obviously is very sensitive to the air–sea exchange formulation, which, however, only affects preformed age, not age^{ideal}. Using an improper gas exchange formulation may hence adversely affect the interpretation of ^{14}C-model experiments concerning a model's circulation dynamics.

One potential solution to this problem is to diagnose the most suitable gas exchange constant for a given model and wind field by performing a bomb-^{14}C calibration experiment (Sweeney et al., 2007). The degree to which this is possible, however, is limited by several methodological problems. The number of ^{14}C ocean data available from early after the atomic bomb testing in the atmosphere, i.e. the 1970s (GEOSECS program, Broecker et

al., 1985; see also Schlitzer, 2015) is small compared with the number of respective data from the 1990s, i.e. from the WOCE and CLIVAR observational programs (Key et al., 2004). The bomb ^{14}C-ocean inventory of the 1970ies is hence less certain than that of the 1990ies. This second time slice, however, may be too late to constrain the adequate gas exchange coefficient of a model independent of the model's ocean circulation (e.g. Graven et al., 2012) as ^{14}C-backfluxes from the ocean to the atmosphere (Naegler, 2009) become increasingly important. The separation of bomb ^{14}C and natural ^{14}C (Rubin and Key, 2002; Sweeney et al. 2007) as well as details of the model implementation of ^{14}C (Mouchet, 2013) add to inevitable uncertainties of a bomb ^{14}C calibration of the gas exchange in a given model.

Ice coverage is another factor potentially influencing the gas equilibration at deep-water formation sites (Ito et al., 2004; Duteil et al., 2013). Ito et al. (2004) reported ice cover to be responsible for about a third of the oxygen disequilibrium observed in their model. In order to study the impact of ice cover on ^{14}C gas exchange and hence preformed ^{14}C-age, we perform one model run with the ECCO-model where ice cover was switched off for 6000 yr. Technically this run was initialized with data from year 4000 of the spin-up and the value of "ice" in Eq. (1) was prescribed to zero. In this experiment preformed ^{14}C-age was reduced by up to 70 yr, or less than 10 % of its normal value (Fig. 8). Ice cover hence appears not to be of major importance in controlling preformed ^{14}C-ages.

Campin et al. (1999) observed differences in the response of $^{14}C\text{-age}^{bulk}$ and age^{ideal} to atmospheric forcing representing the Last Glacial Maximum (LGM) and the present day ocean, respectively. The associated difference of $^{14}C\text{-age}^{pre}$ between LGM and today's ocean has been discussed to be related to an intensified upwelling of ^{14}C-depleted Circumpolar Deep Water (Campin et al., 1999) or an ice-cover induced reduction in ^{14}C-gas exchange during the LGM (Schmittner, 2003). In both studies, ice cover and circulation changed simultaneously, making a direct comparison with our experiments difficult.

4 Case studies

The overall importance, but also the inter-model variability, of the preformed ^{14}C-age is evident from Fig. 9. The preformed ^{14}C-age over much of the ocean contributes to bulk ^{14}C-age by about 50 % in UVIC and ECCO, with higher shares in young water in the upper ocean in all models. In MIT2.8 this fraction is smaller in the deep ocean (about 30 %) (Fig. 9a). In all models, the relative importance of the preformed age component decreases with distance from the deep-water formation regions (Fig. 9b).

Two cases are discussed in the following to demonstrate the adverse effects of neglecting the preformed component of ^{14}C-age we give two examples in the following. For both we make use of a series of model runs to study the sensitivity of ^{14}C-age$^{\text{bulk}}$, age$^{\text{ideal}}$ and the diagnosed preformed ^{14}C-age to the choice of vertical background diffusivity in a model. The intensity of diapycnal mixing in the ocean is one of the key controls of ocean circulation and biogeochemical cycles (Bryan, 1987). For the experimental design we follow Duteil and Oschlies (2011), who used UVIC 2.8. Here, we apply the Kiel-Version of UVIC 2.9 (Keller et al., 2012) to which we added an age$^{\text{ideal}}$ tracer. We perform eight sensitivity runs assuming background mixing coefficients of $K_{\text{vbg}} = 0.01$, 0.05, 0.1, 0.15, 0.2, 0.3, 0.4, 0.5 $\text{cm}^2\,\text{s}^{-1}$. Following Duteil and Oschlies (2011) a value of 1 $\text{cm}^2\,\text{s}^{-1}$ is added to the background diffusivity south of 40° S to account for observed vigorous mixing in the Southern Ocean. Each of the model experiments has been integrated for 10 000 yr under preindustrial atmospheric and astronomical boundary conditions, i.e. all model runs assume constant atmospheric $\Delta^{14}\text{C} = 0$ and $p\text{CO}_2$ of 280 µatm.

In the first example we consider the volume and the age of water in the oxygen minimum zone of the Pacific Ocean. Using UVIC 2.8, Duteil and Oschlies (2011) found dome-shaped distributions for both volume and age with varying K_{vbg}. Maximum suboxic volume and ^{14}C-age$^{\text{bulk}}$ were found at an intermediate K_{vbg} of 0.2 $\text{cm}^2\,\text{s}^{-1}$ (Duteil and Oschlies, 2011, their Fig. 1b). Repeating these experiments with our version of UVIC 2.9, we find a very similar distribution with the ^{14}C-age$^{\text{bulk}}$ maximum also at $K_{\text{vbg}} = 0.2\,\text{cm}^2\,\text{s}^{-1}$ (Fig. 10a). At the highest (lowest) tested K_{vbg} values of 0.5 (0.01) $\text{cm}^2\,\text{s}^{-1}$ the mean bulk ^{14}C-age is

lower by 90 (70) yr. Separating bulk age into its circulation component (age$^{\text{ideal}}$) and its preformed component (^{14}C-age$^{\text{bulk}} - $ age$^{\text{ideal}}$) we find, however, very little sensitivity of age$^{\text{ideal}}$ to K_{vbg} between 0.01 and 0.3. Only for high values of K_{vbg} (0.3 to 0.5 cm^2 s^{-1}) we find that the sensitivity of ^{14}C-age$^{\text{bulk}}$ is mainly due to changes in the circulation component of the age (Fig. 10b). For K_{vbg} values below 0.2 cm^2 s^{-1} more than 60 % of the gradient of ^{14}C-age$^{\text{bulk}}$ (against K_{vbg}) is from the preformed component (Fig. 10c). The similarity of patterns of suboxic volume and ^{14}C-age$^{\text{bulk}}$ led Duteil and Oschlies (2011) to conclude their model results to confirm the notion of a predominant control of suboxic water volume by physical ocean dynamics rather than by local export production and remineralisation. In quantitative terms, and for our model experiments, the suboxic volume appears to be linearly correlated with ^{14}C-age$^{\text{bulk}}$ (Fig. 10d). Variations of ^{14}C-age$^{\text{bulk}}$ explain 65 % (93 %) of the variation of the suboxic volume in the Eastern Tropical Pacific above 1000 m with $n = 8$ ($n = 7$, excluding the lowest value $K_{\text{vbg}} = 0.01$), respectively. In fact, the relationship of suboxic volume and age$^{\text{ideal}}$ is not tight and does not confirm that circulation intensity exerts a simple physical control on the suboxic volume (Fig. 10e). A linear correlation explains about 18 % only of suboxic volume variation by the model's ideal age, i.e. the circulation component of ^{14}C-age. Interpreting ^{14}C-age$^{\text{bulk}}$ as a measure of circulation intensity, i.e. to neglect the preformed component hence yields a faulty assessment of the physical drivers of OMZ volume. Since a local preformed ^{14}C-age always represents the mixing of different surface water end members, the much larger predictive power of ^{14}C-age$^{\text{bulk}}$ (compared with that of age$^{\text{ideal}}$) may alternatively suggest that it is not predominantly circulation intensity (as measured by age$^{\text{ideal}}$) but the combination of different water supply paths (and their variability with K_{vbg}) which control OMZ-volume.

In the second example, which is based on the same model runs, we explore N–S age gradients in the deep Atlantic Ocean. The mean ^{14}C-age$^{\text{bulk}}$ of waters below 1500 m in the Atlantic Ocean shows a marked N–S gradient, with higher values in the Southern Ocean. The slope of this gradient is highly sensitive to the choice of K_{vbg} in the model (Fig. 11a; see also Fig. 3). Ideal age also shows sensitivity to K_{vgb}, but the patterns are very different with highest differences in the tropics and a low sensitivity to K_{vbg} in the northern North

Atlantic but also in the Southern Ocean (Fig. 11b). In fact, the observed patterns are largely due to the differences of the preformed component between model runs (Fig. 11c) with different K_{vbg}. Similar to the OMZ example, patterns of ^{14}C-age$^{\mathrm{bulk}}$ predominantly reflect the mixing of different surface water end members (here the North and South Atlantic end members) to the choice of K_{vbg} and not its impact on circulation intensity (as measured by age$^{\mathrm{ideal}}$). In particular the size of the southern end members of preformed ^{14}C-age vary with the choice of K_{vbg}. In the run with the lowest K_{vbg}, the southern end member of preformed ^{14}C-age (i.e. Southern Ocean surface ^{14}C-age$^{\mathrm{bulk}}$, Fig. 12a–c) is almost twice as high, compared to that of the run with the highest K_{vbg}. In turn, the differences seen in Southern Ocean preformed ^{14}C-age are related to the impact of the chosen value of K_{vbg} on the circulation in the Pacific ocean. With low K_{vbg}, the deep North Pacific shows a ^{14}C-age$^{\mathrm{bulk}}$ of up to 3000 years while with high K_{vbg}, this age is about 1500 yr only (Fig. 14). It is the upwelling of these ^{14}C-depleted waters in the Southern Ocean, which strongly impacts the southern end member of waters ventilating the South Atlantic. The northern end member contributes much less to the K_{vbg} sensitivity of age gradients in the deep Atlantic (Fig. 11). Reading patterns of ^{14}C-age$^{\mathrm{bulk}}$ in the South Atlantic in terms of circulation intensity, i.e. neglecting the differences of preformed ^{14}C-age between runs with different K_{vbg} (which are due to differences in Pacific Ocean circulation in these model runs), would cause a faulty interpretation of the respective model circulation in the Atlantic Ocean.

5 Conclusion

Globally, ^{14}C-age$^{\mathrm{bulk}}$ is dominated by two equally important components, one associated with the time elapsed since last contact with the atmosphere and one associated with a preformed age related to the slow and incomplete equilibration of ^{14}C with atmospheric ^{14}C in the surface ocean. While on average the preformed component accounts for about 50 % of the bulk ^{14}C-age, there is large variability. Regionally, and within a given model, the relative contribution of ^{14}C-age$^{\mathrm{pre}}$ is up to 100 % near the ocean's surface, but is well below 50 % in the oldest deep waters typically observed in the deep North Pacific Ocean. Regional vari-

ability, e.g. in the deep Atlantic Ocean, where it is associated with mixing of end members with very different ^{14}C-age^{pre}, may well mask the circulation component such that it is not visible from the distribution of ^{14}C-age^{bulk}. Between models, the variability can also be considerable, likely due to an interplay of physical model parameters (e.g. diapycnal diffusivity, K_{vbg}) influencing the circulation dynamics within the ocean, and those which control gas exchange of ^{14}C with the atmosphere, like the gas exchange constant, ice coverage, or the wind fields used. In our comparison of three different models the choice of the gas exchange constant (parameter a in Eq. 2) from a parameter range within current uncertainty may either make the UVIC model (Fig. 2a) or the ECCO model (Fig. 7b) to compare most well with observed ^{14}C-age^{bulk}. This is solely due to its impact on the preformed ^{14}C-age component and not related to the circulation of the model in question. A data-based evaluation and tuning of a model's circulation which uses ^{14}C-age^{bulk} without considering the variability of preformed ^{14}C-age is hence at risk to select for the wrong circulation.

In the similar way, temporal changes (e.g. over glacial–interglacial cycles) of the deep ocean ^{14}C-age distributions may be misunderstood if ^{14}C-age^{bulk} is not corrected properly for the preformed component. For paleo-reconstructions the ^{14}C-age^{bulk} of the deep ocean is preserved in the shells of benthic foraminifera and the surface ocean ^{14}C-distribution (i.e. the surface distribution of ^{14}C-age^{pre}) in their pelagic counterparts (Bard, 1988). However, the deep ocean distribution of ^{14}C-age^{pre} is very difficult to quantify since the actual mixing ratios of end members with different ^{14}C-age^{pre} will also change along with a changing circulation (Campin et al., 1999), and it is not well known for time periods other than the present. Model experiments (Campin et al., 1999; Schmittner, 2003) showed that during the last glacial maximum waters in the deep Southern Ocean and South Atlantic appeared to be older (older ^{14}C-age^{bulk}) than in the late Holocene. An increase in Southern Ocean ice cover, which inhibited ^{14}C-gas exchange, was thought to explain much of the apparent age increase (Schmittner, 2003). The actual circulation age as measured by an age^{ideal} tracer, however, was younger in the South Atlantic pointing to a more vigorous circulation (Campin et al., 1999). The shift to older ^{14}C-age^{bulk} in that region was at least partly related to the increased invasion of Antarctic Bottom Water with a large ^{14}C-age^{pre} compared to

that of North Atlantic origin. The relative contribution to high ^{14}C-age^{pre} from (a) the ice-cover related inhibition of ^{14}C-gas exchange (Campin et al., 1999; Schmittner, 2003) and (b) intensified upwelling of old, ^{14}C-depleted, water in the formation region of Antarctic Bottom Water has not been analysed for the last glacial maximum. In the simulations of present-day conditions in our study where the impact of ice cover on ^{14}C-gas exchange was switched off, leaving circulation unchanged, this impact was found to be relatively small (Fig. 9).

The third component of bulk ^{14}C-age, which is associated with the logarithmic decay of ^{14}C, has been quantified in detail in this study. It was found to be generally relatively small, in particular compared to the other two components, which is in agreement with other studies (Holzer et al., 2010; Khatiwala et al., 2012). We propose that in models the preformed component can be estimated from the difference of bulk ^{14}C-age and the model's ideal age (see Eq. 5). There is no straightforward age^{ideal} in the real ocean though. Recent studies have tried to construct an equivalent from a multi-tracer analysis (e.g. Khatiwala et al., 2012). These data products will be very helpful together with the distribution of natural ^{14}C (GLODAP and GLODAP-2) to support data-based model evaluation. Model studies of ocean circulation and biogeochemical processes will benefit from this.

The general form of Eq. (5) is similar to equations describing the principal components of e.g. phosphate and oxygen in the ocean. The observed phosphate concentration at any point in the ocean can be described as the sum of preformed phosphate and phosphate remineralised from decaying organic matter. Similarly, the observed oxygen concentration is the result of preformed oxygen reduced by oxygen consumption from the oxidation of organic matter. It is recognized that model evaluation and inter-comparison benefit from a separation of bulk ocean properties (phosphate, oxygen, alkalinity, etc.) into its preformed components, which return to the ocean's interior through physical transport processes, and the components which result from processing within the ocean (Najjar et al., 2007; Duteil et al., 2012, 2013; Koeve et al., 2014). Based on the results of this study, we propose that considering the preformed ^{14}C-age is equally critical for a meaningful assessment of the circulation of ocean models.

A realistic representation of ocean circulation is a critical aspect of any biogeochemical or carbon cycle model (Gnanadesikan et al., 2004; Doney et al., 2004) since time scales of circulation define how efficiently remineralised nutrients, oxygen deficits or respiratory carbon are stored in the interior ocean. It is only by means of age tracers such as those studied in this work, or CFCs if the upper ocean is concerned, that model circulations and the related time scales of storage can be evaluated against observations. In the case of the ^{14}C-age the interpretation of the observed age-tracer distribution requires an estimate of the ^{14}C-age^{pre}. For the contemporary ocean this is achievable (Matsumoto, 2007; Holzer et al., 2010; Khatiwala et al., 2012). For studies of the paleo-climate this is more difficult but obviously of similar importance (Campin et al., 1999).

Acknowledgements. The Kiel version of the TMM, which we used and modified, was provided by Samar Khatiwala (LDEO, USA) and Iris Kriest (GEOMAR, Germany). The authors acknowledge discussion with H. Dietze and W. Barkmann (GEOMAR, Kiel) and comments from five reviewers and the editor. This study is a contribution to the BIOACID program ("Biological Impacts Of Ocean Acidification") funded by BMBF (FKZ 03F0608A) (W. Koeve). We received additional funding from the EU FP7 project CARBOCHANGE ("Changes in carbon uptake and emissions by oceans in a changing climate"; Grant agreement no. 264879) (H. Wagner and A. Oschlies) and the Deutsche Forschungsgemeinschaft (SFB 754) (P. Kähler and A. Oschlies).

References

Adkins, J. F. and Boyle, E. A.: Changing atmospheric Δ^{14}C and the record of deep water paleoventilation ages, Paleoceanography, 12, 337–344, 1997.

Bard, E.: Correction of accelerator mass spectrometry ^{14}C ages measured in planktonic foraminifera, Paleoceanography, 3, 635–645, 1988.

Bitz, C. M., Holland, M. M., Weaver, A. J., and Eby, M.: Simulating the ice-thickness distribution in a coupled climate model, J. Geophys. Res., 106, 2441–2463, 2001.

Bolin, B. and Rohde, H.: A note on the concepts of age distribution and residence time in natural reservoirs, Tellus, 25, 58-62.

Broecker, W. S.: A revised estimate for the radiocarbon age of North Atlantic Deep Water, J. Geophys. Res., 84, 3218–3226, 1979.

Broecker, W. S. and Peng, T.-H.: Gas exchange rates between air and sea, Tellus, 26, 21–35, 1974.
Broecker, W. S. and Peng, T.-H.: Tracers in the Sea, Columbia University, Palisades, 690 pp., 1982.
Broecker, W. S., Peng., T.-H., Ostlund, H. G., and Stuiver, M.: The distribution of bomb radiocarbon in the ocean, J. Geophys. Res., 90, 6953–6970, 1985.
Broecker, W.S.; Blanton, S.; Smethie, W.M.Jr., Ostlund, G.: Radiocarbon decay and oxygen utilization in the deep Atlantic ocean, Global Biogeochem. Cycles, 5, 87-117, 1991.
Bryan, F.: Parameter sensitivity of primitive equation ocean general circulation models, J. Phys. Oceanogr., 17, 970–985, 1987.
Caldeira, K., Wickett, M. E., and Duffy, P. B.: Depth, radiocarbon, and the effectiveness of direct CO_2 injections as an ocean carbon sequestration strategy, Geophys. Res. Lett., 29, 1766, doi:10.1029/2001GL014234, 2002.
Campin, J.-M., Fichefet, T., and Duplessy, J.-C.: Problems with using radiocarbon to infer ocean ventilation rates for past and present climates, Earth Planet. Sc. Lett., 165, 17–24, 1999.
Cao, L. and Jain, A.: An Earth system model of intermediate complexity: simulations of the role of ocean mixing paramerizatioins and climate change in estimated uptake for natural and bomb radiocarbon and anthropogenic CO_2, J. Geophys. Res., 110, C09002, doi:10.1029/2005JC002919, 2005.
Deleersnijder, E., Campin, J.-M., and Delhez, E.J.M.: The concept of age in marine modelling. I. Theory and preliminary model results, J. Mar. Syst., 28, 229-267, 2001.
Delhez, E.J.M., Deleersnijder, E., Mouchet, A., and Beckers, J.-M.: A note on the age of radioactive tracers, J. Mar. Syst., 38, 277-286, 2003.
Delhez, E.J.M., Heemink, A.W., Deleersnijder, E.: Residence time in a semi-enclosed domain from the solution of an adjoint problem Estuar. Coast. Shelf Sci, 61, 691-702.
DeVries, T. and Primeau, F.: Dynamically and observationally constrained estimates of water-mass distributions and ages in the global ocean, J. Phys. Oceanogr., 41, 2381–2401, doi:10.1175/JPO-D-10-05011.1, 2011.
Doney, S.C.; Lindsay, K.; Caldeira, K.; Campin, J.-M.; Drange, H.; Dutay, J.-C.; Follows, M.; Gao, Y.; Gnanadesikan, A.; Gruber, N.; Ishida, A.; Joos, F.; Madec, G.; Maier-Reimer, E.; Marschall, J.C.; Matear, R.J.; Monfray, P.; Mouchet, A.; Najjar, R.; Orr, J.C.; Plattner, G.-K.; Sarmiento, J.; Schlitzer, R.; Slater, R.; Totterdell, I.J.; Weirig, M.-F.; Yamanaka, Y.; Yool, A.: Evaluating global ocean carbon models: the importance of realistic physics, Global Biogeochem Cy, 18, GB3017, doi:10.1029/2003GB002150, 2004.

Druffel, E. M.: Radiocarbon in annual coral rings from the eastern tropical pacific ocean, Geophys. Res. Lett, 8, 59–62, 1981.

Duteil, O. and Oschlies, A.: Sensitivity of simulated extent and future evolution of marine suboxia to mixing intensity, Geophys. Res. Lett., 38, L06607, doi:10.1029/2011GL046877, 2011.

Duteil, O., Koeve, W., Oschlies, A., Aumont, O., Bianchi, D., Bopp, L., Galbraith, E., Matear, R., Moore, J. K., Sarmiento, J. L., and Segschneider, J.: Preformed and regenerated phosphate in ocean general circulation models: can right total concentrations be wrong?, Biogeosciences, 9, 1797–1807, doi:10.5194/bg-9-1797-2012, 2012.

Duteil, O., Koeve, W., Oschlies, A., Bianchi, D., Galbraith, E., Kriest, I., and Matear, R.: A novel estimate of ocean oxygen utilisation points to a reduced rate of respiration in the ocean interior, Biogeosciences, 10, 7723–7738, doi:10.5194/bg-10-7723-2013, 2013.

Emerson, S. R. and Hedges, J. I.: Chemical Oceanography and the Marine Carbon Cycle, Cambridge University Press, Cambridge, 453 pp., 2008.

England, M. H.: The age of water and ventilation timescales in a global ocean model, J. Phys. Oceanogr., 25, 2756–2777, 1995.

England, M. H. and Maier-Reimer, E.: Using chemical tracers to assess ocean models, Rev. Geophys., 39, 29–70, 2001.

Feely, R. A., Sabine, C. L., Lee, K., Millero, F. J., Lamb, M. F., Greeley, D., Bullister, J. L., Key, R. M., Peng, T.-H., Kozyr, A., Ono, T., and Wong, C. S.: In situ calcium carbonate dissolution in the Pacific Ocean, Global Biogeochem. Cy., 16, 1144, doi:10.1029/2002GB001866, 2002.

Fiadeiro, M. E.: Three-dimensional modeling of tracers in the deep Pacific Ocean II. Radiocarbon and the circulation, J. Mar. Res., 40, 537–550, 1982.

Follows, M. J., Ito, T., and Dutkiewicz, S.: On the solution of the carbonate chemistry system in the ocean biogeochemistry models, Ocean Model., 12, 290–301, 2006.

Franke, J., Schulz, M., Paul, A., and Adkins, J. F.: Assessing the ability of the ^{14}C projection-age method to constrain the circulation of the past in a 3-D ocean model, Geochem. Geophy. Geosy., 9, Q08003, doi:10.1029/2008GC001943, 2008a.

Franke, J., Paul, A., and Schulz, M.: Modeling variations of marine reservoir ages during the last 45 000 years, Clim. Past, 4, 125–136, doi:10.5194/cp-4-125-2008, 2008b.

Gnanadesikan, A., Dunne, J.P., Key, R.M., Matsumoto, K., Sarmiento, J.L., Slater, R.D., Swathi, P.S Oceanic ventilation and biogeochemical cycling: understanding the physical mechanisms that produce realistic distributions of tracers and productivity, Global Biogeochem. Cy, 18, GB4010, do:10.1029/2003GB002097, 2004.

Graven, H.D., Gruber, N., Key, R., Khatiwala, S., and Giraud, X.: Changing controls on oceanic radiocarbon: new insights on shallow-to-deep ocean exchange and anthropogenic CO_2-uptake, J. Geophys. Res., 117, C10005, doi:10.10.29/2012JC008074, 2012.

Holzer, M., Primeau, F.W., Smethie, Jr. W.M., and Khatiwala, S. : Where and how long ago was water in the western North Atlantic ventilated? Maximum-entropy inversions of bottle data from WOCE line A20, J. Geophys. Research, 115, C07005, doi:10.1029/2009JC005750, 2010.

Ito, T., Follows, M. J., and Boyle, E. A.: Is AOU a good measure of respiration in the ocean?, Geophys. Res. Lett., 31, L17305, doi:10.1029/2004GL020900, 2004.

Jahn, A., Lindsay, K., Giraud, X., Gruber, N., Otto-Bliesner, B.L., Liu, Z., and Brady, E.C.: Carbon isotopes in the ocean model of the Community Earth System Model (CESM1), Geosci. Model Dev. Discuss., , 7261-7503, 2014.

Jain, A. K., Khesgi, H. S., Hoffert, M. I., and Wuebbles, D. J.: Distribution of radiocarbon as a test of global carbon cycle models, Global Biogeochem. Cy., 9, 153–166, 1995.

Jenkins, W.J.: ^{3}H and ^{3}He in the Beta Triangle: Observations of gyre ventilation and oxygen utilization rates, J. Phys. Oceanogr., 17, 763-783, 1987.

Key, R. M., Kozyr, A., Sabine, C. L., Lee, K., Wanninkhof, R., Bullister, J. L., Feely, R. A., Millero, F. J., Mordy, C., and Peng, T.-H.: A global ocean carbon climatology: results from Global Data Analysis Project (GLODAP), Global Biogeochem. Cy., 18, GB4031, doi:10.1029/2004GB002247, 2004.

Khatiwala, S.: A computational framework for simulation of biogeochemical tracers in the ocean, Global Biogeochem. Cy., 21, GB3001, doi:10.1029/2007GB002923, 2007.

Khatiwala, S., Visbeck, M., and Schlosser, P.: Age tracers in an ocean GCM, Deep-Sea Res. Pt. I, 48, 1432–1441, 2001.

Khatiwala, S., Visbeck, M., and Cane, M. A.: Accelerated simulation of passive tracers in ocean circulation models, Ocean Model., 9, 51–69, 2005.

Khatiwala, S., Primeau, F., and Holzer, M.: Ventilation of the deep ocean constrained with tracer observations and implications for radiocarbon estimates of ideal mean age, Earth Planet. Sc. Lett., 325, 116–125, 2012.

Keller, D. P., Oschlies, A., and Eby, M.: A new marine ecosystem model for the University of Victoria Earth System Climate Model, Geosci. Model Dev., 5, 1195–1220, doi:10.5194/gmd-5-1195-2012, 2012.

Koeve, W., Duteil, O., Oschlies, A., Kähler, P., and Segschneider, J.: Methods to evaluate $CaCO_3$ cycle modules in coupled global biogeochemical ocean models, Geosci. Model Dev., 7, 2393–2408, doi:10.5194/gmd-7-2393-2014, 2014.

Kriest, I., Khatiwala, S., and Oschlies, A.: Towards and assessment of simple global marine biogeochemical models of different complexity, Prog. Oceanogr., 86, 337–360, 2010.

Kriest, I., Oschlies, A., and Khatiwala, S.: Sensitivity analysis of simple global marine biogeochemical models, Global Biogeochem. Cy., 26, GB2029, doi:10.1029/2011GB004072, 2012.

Lynch-Stieglitz, J.: Tracers of past ocean circulation, in: Treatise on Geochemistry, 6, 433–451, 2003.

Marshall, J. and Speer, K.: Closure of the meridional overturning circulation through Southern Ocean upwelling, Nat. Geosci., 5, 171–180, doi:10.1038/NGEO1391, 2012.

Marshall, J., Adcroft, A., Hill, C., Perelman, L., and Heisey, C.: A finite-volume, incompressible navier-stokes model for studies of the ocean on parallel computers, J. Geophys. Res., 102, 5733–5752, 1997.

Matsumoto, K.: Radiocarbon-based circulation age of the world ocean, J. Geophys. Res., 112, C09004, doi:10.1029/2007JC004095, 2007.

Matsumoto, K., Sarmiento, J. L., Key, R. M., Aumont, O., Bullister, J. L., Caldeira, K., Campin, J.-M., Doney, S. C., Drange, H., Dutay, J.-C., Follows, M., Gao, Y., Gnanadesikan, A., Gruber, N., Ishida, A., Joos, F., Lindsay, K., Maier-Reimer, E., Marshall, J. C., Matear, R. J., Monfray, P., Mouchet, A., Najjar, R., Plattner, G.-K., Schlitzer, R., Slater, R., Swathi, P. S., Totterdell, I. J., Weirig, M.-F., Yamanaka, Y., Yool, A., and Orr, J. C.: Evaluation of ocean carbon cycle models with data-based metrics, Geophys. Res. Lett., 31, L07303, doi:10.1029/2003GL018970, 2004.

Mouchet, A.: The ocean bomb radiocarbon inventory revisited, Radiocarbon, 55, 1580-1594, 2013.

Naegler, T.: Reconciliation of excess $\Delta^{14}C$-constrained global CO_2 piston velocity estimates, Tellus B, 61, 372-384, doi: 10.1111/j.600-0889.2008.00408.x, 2009.

Najjar, R. G., Jin, X., Louanchi, F., Aumont, O., Caldeira, K., Doney, C. S., Dutay, J.-C., Follows, M., Gruber, N., Joos, F., Lindsay, K., Maier-Reimer, E., Matear, R. J., Matsumoto, K., Monfray, P., Mouchet, A., Orr, J. C., Plattner, G.-K., Sarmiento, J. L., Schlitzer, R., Slater, R. D., Wierig, M.-F., Yamanaka, Y., and Yool, A.: Impact of circulation on export production, dissolved organic matter, and dissolved oxygen in the ocean: results from phase II of the Ocean Carbon-cycle Model Intercomparison Project (OCMIP-2), Global Biogeochem. Cy., 21, GB3007, doi:10.1029/2006GB002857, 2007.

Orr, J., Najjar, R., Sabine, C. L., and Joos, F.: Abiotic-HOWTO. Internal OCMIP Report, LSCE/CEA Saclay, Gif-sur-Yvette, France, 25 pp.,revision: 1.16, available at: http://ocmip5.ipsl.jussieu.fr/OCMIP/phase2/simulations/Abiotic/HOWTO-Abiotic.html (last access: 28 November 2013), 2000.

Oschlies, A., Schulz, K. G., Riebesell, U., and Schmittner, A.: Simulated 21st century's increase in oceanic suboxia by CO_2-enhanced biotic carbon export, Global Biogeochem. Cy., 22, GB4008, doi:10.1029/2007GB003147, 2008.

Rafter, T. A. and Fergusson, G. J.: Atom bomb effect – recent increase of carbon-14 content of the atmosphere and the biosphere, Science, 126, 557–558, 1957.

Redfield, A. C., Ketchum, B. H., and Richards, F. A.: The influence of organisms on the composition of seawater, in: The Sea, Vol. 2, edited by: Hill, M. N., John Wiley & Sons, New York, 26–77, 1963.

Rubin, S. I. and Key, R. M.: Separating natural and bomb-produced radiocarbon in the ocean: the potential alkalinity method, Global Biogeochem. Cy., 16, 1105, doi:10.1029/2001GB001432, 2002.

Sarmiento, J. L., Thiele, G., Key, R. M., and Moore, W. S.: Oxygen and nitrate new production and remineralization in the North Atlantic subtropical gyre, J. Geophys. Res., 95, 18303–18315, 1990.

Schlitzer, R.: Geochemical Ocean Sections Program - GEOSECS, Hydrographic and Tracer Data, ODV Dataset, http://odv.awi.de/en/data/ocean/geosecs/, last accessed: 21.05.2015, 2015.

Schmittner, A.: Southern Ocean sea ice and radiocarbon ages of glacial bottom water, Earth Planet. Sc. Lett., 213, 53-62, 2003.

Schmittner, A., Oschlies, A., Matthews, H. D., and Galbraith, E. D.: Future changes in climate, ocean circulation, ecosystems, and biogeochemical cycling simulated for a business-as-usual CO_2 emission scenario until year 4000 AD, Global Biogeochem. Cy., 22, GB1013, doi:10.1029/2007GB002953, 2008.

Stammer, D., Ueyoshi, K., Köhl, A., Large, W. G., Josey, S. A., and Wunsch, C.: Estimating air–sea fluxes of heat, freshwater, and momentum through global ocean data assimilation, J. Geophys. Res., 109, C05023, doi:10.1029/2003JC002082, 2004.

Stuiver, M.: ^{14}C distribution in the Atlantic Ocean, J. Geophys. Res., 85c, 2711–2718, 1980.

Stuiver, M. and Polach, H. A.: Reporting of ^{14}C data, Radiocarbon, 19, 355–363, 1977.

Stuiver, M., Quay, P. D., and Ostlund, H. G.: Abyssal water carbon-14 distribution and the age of the word ocean, Science, 219, 849–851, 1983.

Suess, H.: Radiocarbon concentration in modern wood, Science, 122, 415–417, 1955.

Sweeney, C., Gloor, E., Jacobson, A. R., Key, R. M., McKinley, G., Sarmiento, J. L., and Wanninkhof, R.: Constraining global air–sea gas exchange for CO_2 with recent bomb ^{14}C measurements, Global Biogeochem. Cy., 21, GB2015, doi:10.1029/2006GB002784, 2007.

Takeoka, H.: Fundamental concepts of exchange and transport time scales in a coastal sea, Cont. Shelf Res., 3, 311-326.

Thiele, G. and Sarmiento, J. L.: Tracer dating and ocean ventilation, J. Geophys. Res., 95, 9377–9391, 1990.

Toggweiler, J. R., Dixon, K., and Bryan, K.: Simulations of radiocarbon in a coarse-resolution world ocean model. 1. steady state prebomb distribution, J. Geophys. Res., 94, 8217–8242, 1989.

Trenberth, K. E., Large, W. G., and Olson, J. G.: A Global Ocean Wind Stress Climatology Based on ECMWF Analyses, National Center for Atmospheric Research, 93 pp., 1989.

Weaver, A. J., Eby, M., Wiebe, E. C., Bitz, C. M., Duffy, P. B., Ewen, T. L., Fanning, A. F., Holland, M. M., MacFadyen, A., Matthews, H. D., Meissner, K. J., Saenko, O., Schmittner, A., Wang, H., and Yoshimori, M.: The UVIC earth system climate model: model description, climatology, and applications to past, present and future climates, Atmos. Oceans, 39, 361–428, 2001.

Table 1. Tracers.

Tracer name	Age name	Source/sink	Sea-surface B.C.	Component	Comments
^{14}C-DIC^{decay}	^{14}C-age^{decay}	radioactive decay	0	Circulation	(1)
^{14}C-DIC^{pre}	^{14}C-age^{pre}	none	^{14}C-DIC^{bulk}	Preformed	(1)
^{14}C-DIC^{bulk}	^{14}C-age^{bulk}	radioactive decay	Equ 1b	Total	(1)
age^{ideal}	age^{ideal}	aging	0	Circulation	(2)
age^{pre}	age^{pre}	none	^{14}C-age^{bulk}	Preformed	(2)
age^{bulk}	age^{bulk}	aging	^{14}C-age^{bulk}	Total	(2)

(1) ^{14}C-ages: subject to non-linear mixing effect (2) Ages: not subject to non-linear mixing effect

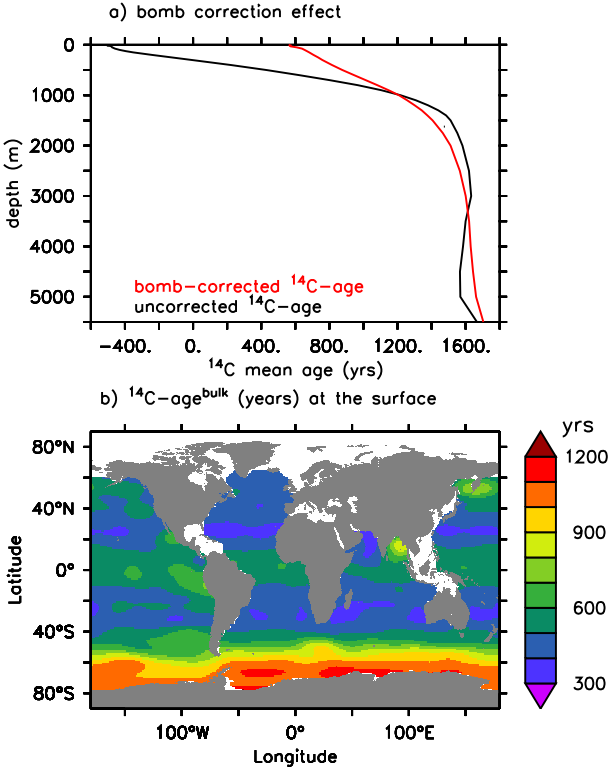

Figure 1. (a) Global mean profiles (GLODAP) of bulk ^{14}C-age (red) and the pseudo age of ^{14}C-DIC not corrected for the effects of bomb and anthropogenic ^{14}C signatures. **(b)** Map of bulk ^{14}C-age at the surface of the Ocean (GLODAP).

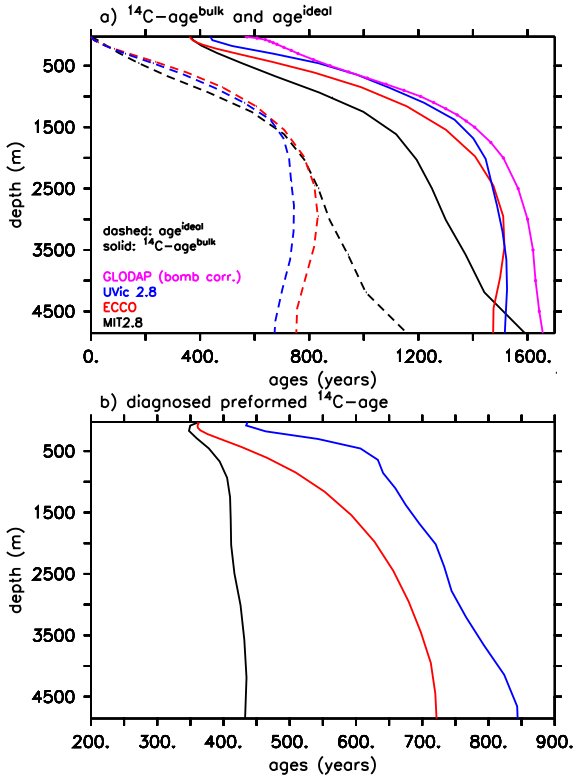

Figure 2. (a) Global mean profiles of bulk ^{14}C-age (solid lines) and ideal age (dashed lines) for three different global ocean circulation models (color code see figure insert) and the GLODAP database (solid magenta). **(b)** Global mean profiles of the difference between bulk ^{14}C-age and ideal age for three different global ocean circulation models (colour code as **a**).

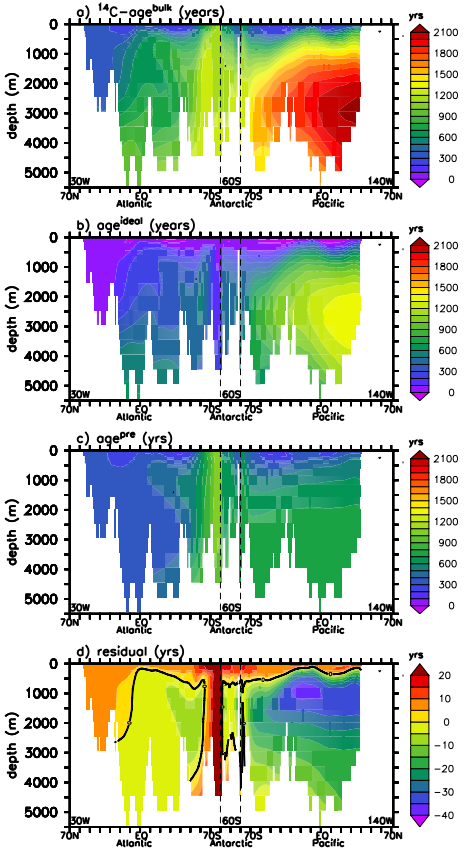

Figure 3. Bulk ^{14}C-age **(a)**, ideal age **(b)** and preformed age **(c)** from the ECCO experiment along a combined section through the North Atlantic (30° W), the Southern Ocean (60° S), and the Pacific Ocean (140° W). The preformed age is taken from the age^{pre} tracer (see Sect. 2.2 for tracer definition). **(d)** shows the residual (^{14}C-age^{bulk} − age^{ideal} − age^{pre}), i.e. the third term on the right hand side of Eq. (4).

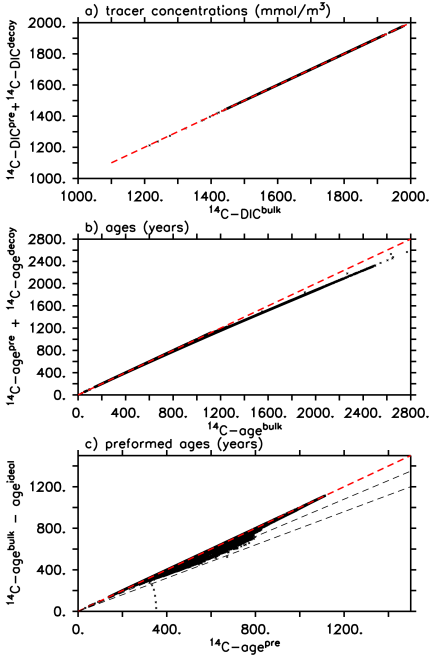

Figure 4. Scatter plots **(a)** of ^{14}C-DIC tracer concentrations vs. the sum of ^{14}C-DIC^{pre} and ^{14}C-DIC^{decay} tracer concentrations and **(b)** bulk ^{14}C-age vs. the sum of ages computed from ^{14}C-DIC preformed and decay tracers. Note that a few grid cells with ^{14}C-DIC concentrations below about 1300 mmol m^{-3} and bulk ages above about 2600 yr are not fully in steady state after the 2500 yr run time of this model experiment. We ignore these grid cells in the discussion. **(c)** Comparison of ages derived from the ^{14}C-DIC preformed tracer and by difference of the bulk ^{14}C-DIC tracer and the ideal age tracer. Red dashed line is the 1 : 1 line, dashed grey lines indicate −10 and −20 % isolines.

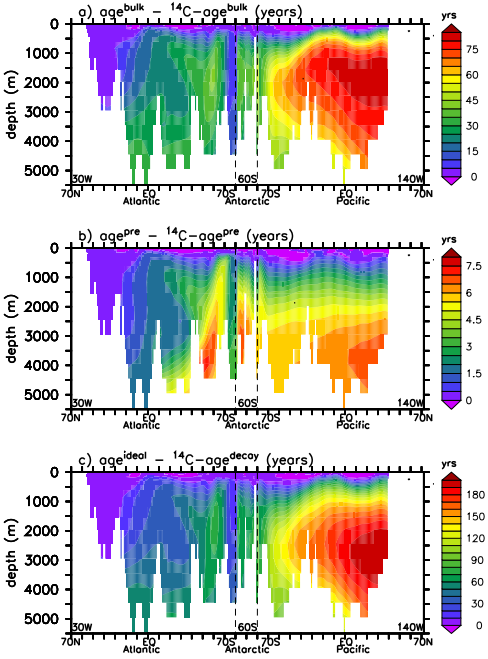

Figure 5. Anomalies (ideally behaving tracer $-$ ^{14}C-based tracer) of bulk age **(a)**, preformed component of age **(b)** and circulation component of age **(c)**.

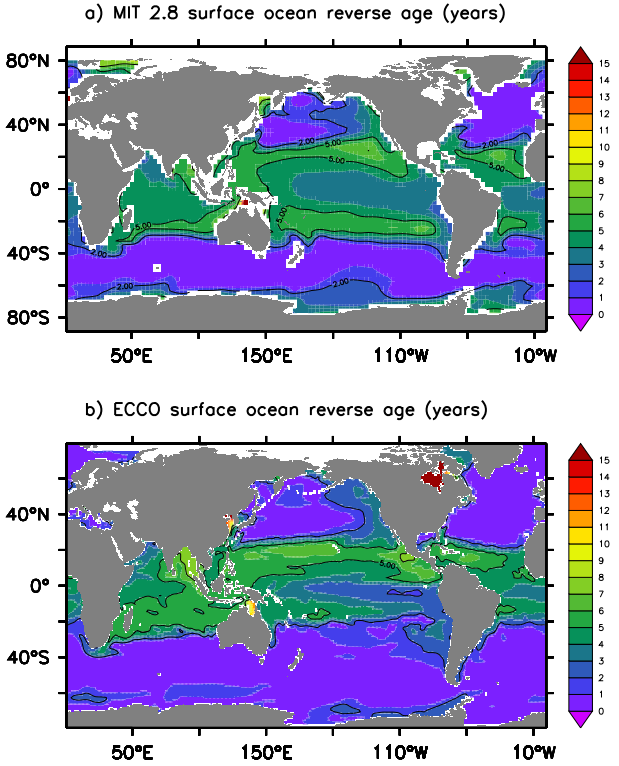

Figure 6. Surface ocean reverse age (yr) computed for the MIT2.8 **(a)** and ECCO **(b)** model.

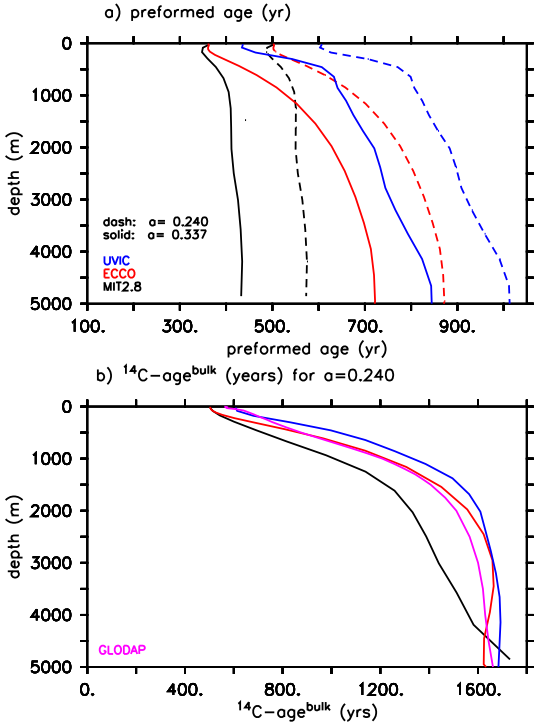

Figure 7. Sensitivity of preformed and bulk ^{14}C-age to the choice of the gas exchange parameter a of Eq. (1). **(a)** preformed ^{14}C-age for $a = 0.337$ (solid lines) and $a = 0.24$ (dashed lines). Results from MIT2.8 (black), ECCO (red), and UVIC (blue) are shown. **(b)** Global mean profiles of ^{14}C-age$^{\text{bulk}}$ using $a = 0.24$.

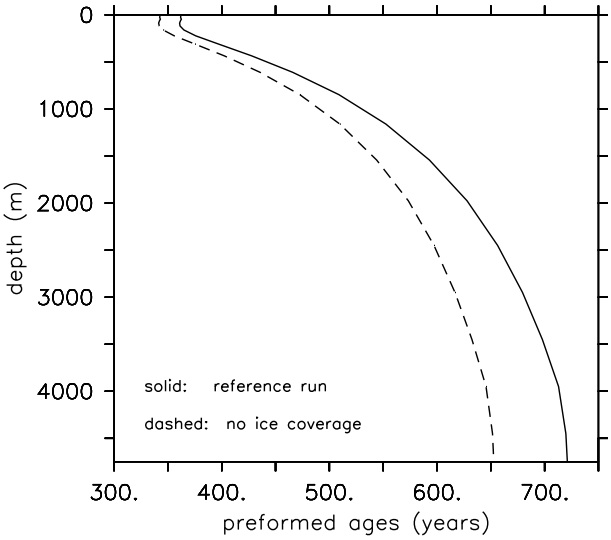

Figure 8. Sensitivity of preformed ^{14}C-age to ice cover. Solid line: control with ice cover affecting CO_2 gas exchange, dashed: effect of ice cover on CO_2 gas exchange ignored. Results are from the ECCO model, both runs use identical circulation.

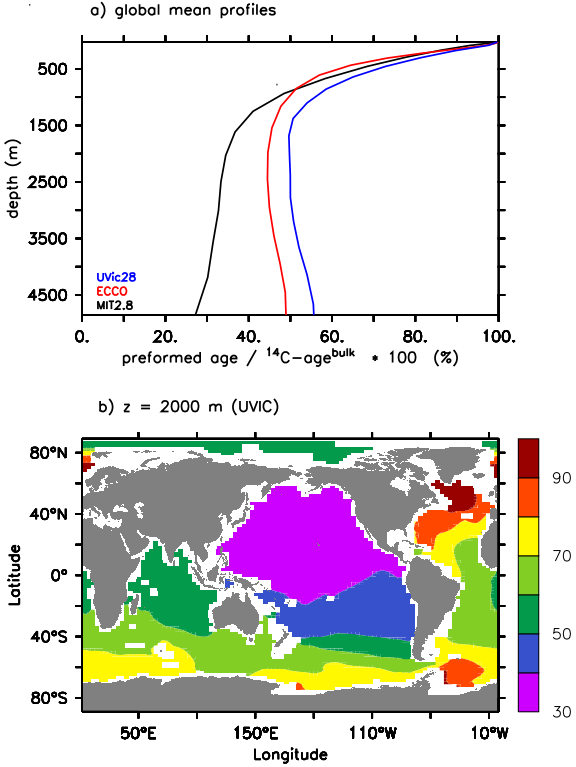

Figure 9. (a) Global mean profiles of the relative contribution (%) of preformed age (estimated as bulk ^{14}C-age − ideal age) to the bulk ^{14}C-age. **(b)** As Fig. 9a, but for the UVIC model in 2000 m depths, displaying that even in the oldest waters of the North Pacific the preformed age is a significant component of the bulk age.

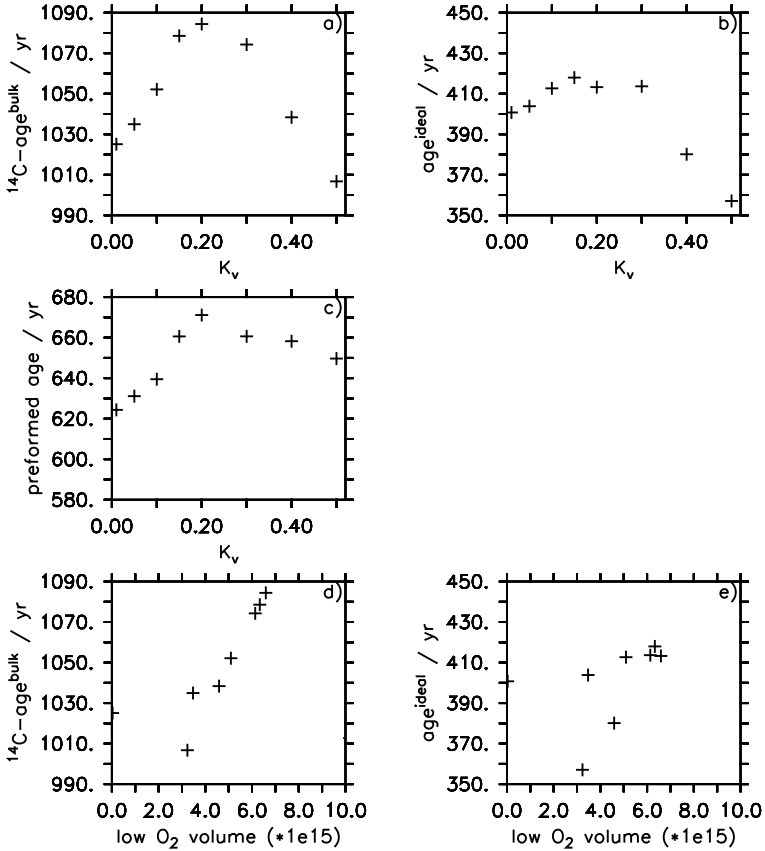

Figure 10. Sensitivity of ages of suboxic waters to vertical diffusivity (K_{vbg}) in the UVIC model. **(a)** Bulk age, **(b)** ideal age, **(c)** preformed age. Scatterplots of bulk age **(d)** and ideal age **(e)** vs. volume of suboxic waters in the model runs.

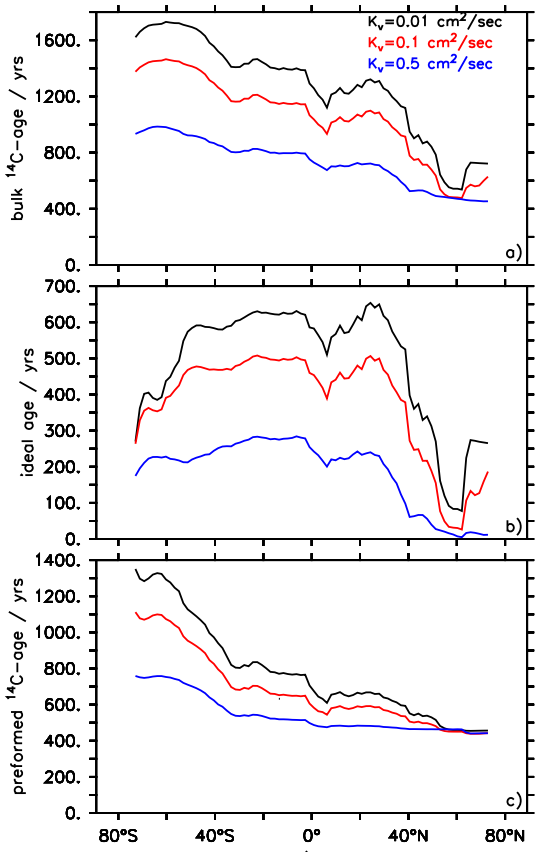

Figure 11. Sensitivity of Atlantic Ocean age patterns to vertical diffusivity (K_{vbg}) in the UVIC model. **(a)** Bulk ^{14}C-age, **(b)** ideal age, **(c)** preformed ^{14}C-age. Preformed ^{14}C-age is diagnosed here from the difference of bulk age and ideal age.

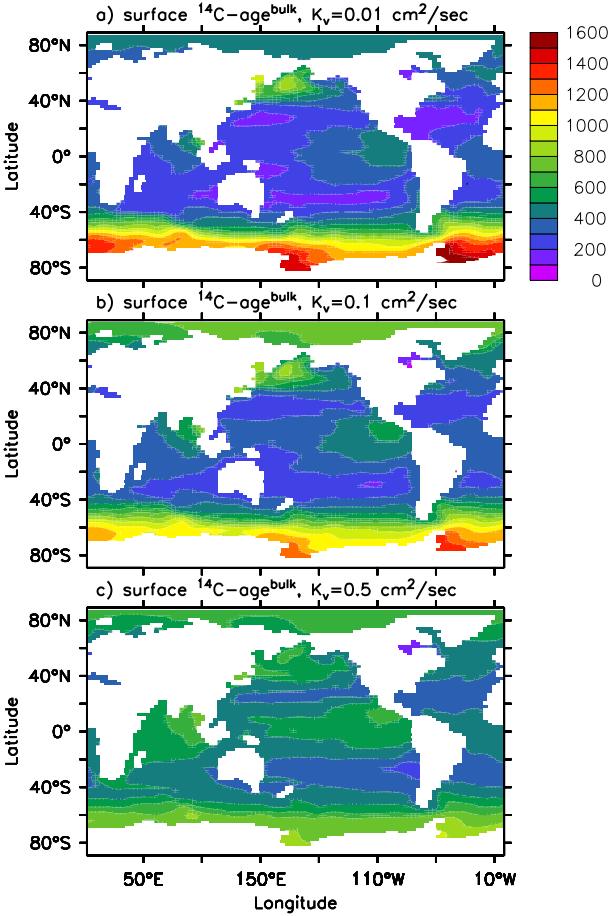

Figure 12. Surface bulk ^{14}C-age in the UVIC model for three different K_{vbg} values. **(a)** $K_{\text{vbg}} = 0.01\,\text{cm}^2\,\text{s}^{-1}$, **(b)** $K_{\text{vbg}} = 0.1\,\text{cm}^2\,\text{s}^{-1}$ and **(c)** $K_{\text{vbg}} = 0.5\,\text{cm}^2\,\text{s}^{-1}$.

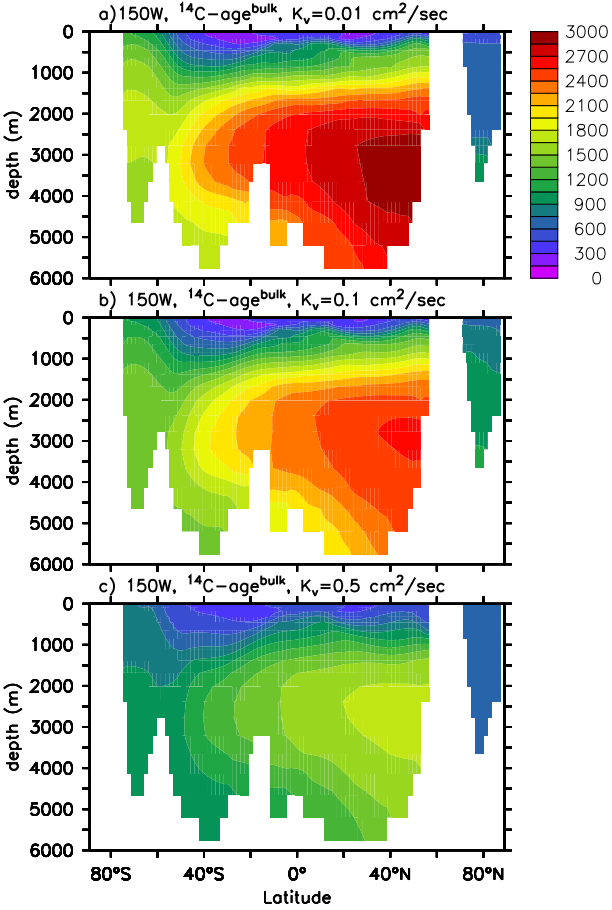

Figure 13. Vertical section along 150° W of bulk ^{14}C-age in the UVIC model for three different K_{vbg} values. **(a)** $K_{\mathrm{vbg}} = 0.01\,\mathrm{cm^2\,s^{-1}}$, **(b)** $K_{\mathrm{vbg}} = 0.1\,\mathrm{cm^2\,s^{-1}}$ and **(c)** $K_{\mathrm{vbg}} = 0.5\,\mathrm{cm^2\,s^{-1}}$.